Direct Correlation between Donor-Acceptor Distance and Temperature Dependence of Kinetic Isotope Effects in Hydride-Tunneling Reactions of NADH/NAD$^+$ Analogues

Mingxuan Bai, Shailendra Koirala, Yun Lu*

Department of Chemistry, Southern Illinois University Edwardsville, Edwardsville, IL 62026, United States

Supporting Information Placeholder

ABSTRACT: Recent study of structural effects on primary kinetic isotope effects (1° KIEs) of H-transfer reactions in enzymes and solution revealed that a more rigid reaction system gave rise to a weaker temperature dependence of 1° KIEs, *i.e.*, a smaller isotopic activation energy difference ($\Delta E_a = E_{aD} - E_{aH}$). This has been explained within the contemporary vibrationally assisted activated H-tunneling (VA-AHT) model in which rigidity is defined according to the density of donor-acceptor distance (DAD_{TRS}) populations at the tunneling ready state (TRS) sampled by heavy atom motions. To test the relationship between DAD_{TRS} and ΔE_a in the model, we developed a computational method to obtain the TRS structures for H-transfer reactions. The method was applied to three hydride transfer reactions of NADH/NAD$^+$ analogues for which the ΔE_a's as well as secondary (2°) KIEs have been reported. The 2° KIEs computed from each TRS structure were fitted to the observed values to obtain the optimal TRS's/DAD_{TRS}'s. It was found that a shorter DAD_{TRS} does correspond with a smaller ΔE_a. This appears to support the VA-AHT model. Moreover, an analysis of hybridizations at the bent TRS structures shows that rehybridizations at the donor-acceptor centers are much more advanced than predicted from the classical mechanism. This implicates that more orbital preparations are required for the nonclassical H-tunneling to take place.

Introduction

Experimental evidence for H-tunneling effect has largely come from the study of hydrogen kinetic isotope effects (KIEs). Within the semi-classical transition state (TS) theory, a primary (1°) deuterium (D) KIE is predicted to range from 2 to 9. When 1° KIE is larger than 9, H-tunneling mechanism is generally suggested, which has been described in the traditional Bell model that adds a tunnel correction to the "static" classical energy barrier.[1] In addition to KIE's size, its temperature dependency, characterized by the isotopic activation energy difference ($\Delta E_a = E_{aD} - E_{aH}$), has also been used to suggest H-tunneling, which is when ΔE_a is outside of the semi-classical range of 1.0 – 1.2 kcal/mol.[2,3] In the past two decades, however, many observations were found unexplainable by the Bell model. Those could include but not be limited to (1) the 1° KIE and ΔE_a values being not outside of their respective semi-classical limits at the same time,[4-6] (2) the huge 1° KIEs at room temperature conditions,[7,8] as well as (3) the temperature independence of 1° KIEs ($\Delta E_a = 0$) determined at room temperature conditions.[9-12] Contemporary H-tunneling models that involve heavy atom motions to mediate H-tunneling have been proposed to attempt to explain the "abnormal" KIE results, but none has been largely accepted so far.[12-14] While the oversimplified Bell model is currently still largely used to explain KIEs in the scientific field,[15,16] and there is extensive debate as to which contemporary model is most appropriate to explain H-transfer/tunneling chemistry,[13,14,17,18] research efforts are needed to put forth a universally accepted H-transfer/tunneling model. Finding such a model would benefit from the *systematic* study of structure – 1° KIE – ΔE_a relationship, but that, especially the structure – ΔE_a relationship, has not received enough attentions so far.

To our knowledge, the relatively *systematic* study of the structure – ΔE_a relationship for H-transfer reactions was not started until 20 years ago when temperature independence of KIEs ($\Delta E_a \approx 0$) was frequently observed in the wild-type enzymes, but temperature dependence of KIEs ($\Delta E_a > 0$) to different extents was found in enzyme variants.[9,11,12,19-32] The former cannot be explained by Bell model, simply because $\Delta E_a \approx 0$ is an extreme case in the model for which $E_{aH} = E_{aD}$ are supposed to be close to 0 and KIE to be huge, which could only happen at extremely low temperature conditions.[1] Contemporary vibrationally assisted activated H-tunneling (VA-AHT) model, initially proposed by Klinman and coworkers[11,12,18] on the basis of the work of Kuznetsov–Ulstrup[33] and used and developed by several other groups,[29,31,34-36] was applied to explain the observations. According to that model, the tunneling-ready state (TRS) has fluctuating donor(D)-acceptor(A) distances (DAD_{TRS}'s) sampled by the thermal motions of heavy atoms, and H-wavefunction overlap (H-tunneling) occurs between the potential wells of the degenerate reactant $[D\text{-}H]^{\neq}$ and product $[H\text{-}A]^{\neq}$ moieties in the TRS ($[D\text{-}H\text{---}H\text{-}A]^{\neq}$) of different DAD_{TRS}'s.[37,38] (In $[D\text{-}H\text{---}H\text{-}A]^{\neq}$, H is in a quantum state being at both sides of the reactant and product simultaneously.) Since the tunneling process is wave-packet density (or wavelength) sensitive and thus H-isotope sensitive, 1° KIE is defined to be the ratio of isotopic wavefunction overlaps over all of the DAD_{TRS}'s sampled. (Since H-overlap is greater than D-overlap, 1° KIE > 1.) Since this ratio changes with DAD_{TRS}, temperature dependence of DAD_{TRS}'s reflects temperature dependence of 1° KIEs. Therefore, the wild-type enzyme protein structures are generally well packed with constructive vibrations (heavy atom motions) to make densely populated DAD_{TRS}'s or rigid reaction centers leading to weak temperature dependence of both DAD_{TRS}'s and 1° KIEs. When mutagenesis is made on the hydrophobic side chains, the naturally evolved well packed proteins and constructive vibrations are impaired most likely broadening the DAD_{TRS} distributions making DAD_{TRS}'s and KIEs more susceptible to temperature change. While these 1° KIE observations in enzymes appear to be well

explained by the new VA-AHT model, further systematic studies of the $DAD_{TRS} - \Delta E_a$ relationship for general H-transfer reactions are needed to test the explanations and the model. As a matter of fact, we have studied the structure – ΔE_a relationship for several hydride transfer reactions in solution and concluded that the more rigid reaction centers with more densely distributed DAD_{TRS}'s gave rise to a smaller ΔE_a value, supporting the predicted $DAD_{TRS} - \Delta E_a$ relationship in the model and explanations for the observations in enzymes.[39,40] It should be noted, however, that the other contemporary H-tunneling model or other methods of simulation of H-tunneling have also been attempted to explain above KIE observations in enzymes, and sometimes similar DAD_{TRS} explanations were resulted,[41-44] but only the VA-AHT model is able to predict such a relationship beforehand.[18,36]

Above explanations using the effect of DAD_{TRS} on ΔE_a for H-transfer reactions within the VA-AHT model are only qualitative as the real DAD information at the TRS, i.e., DAD_{TRS}, has remained elusive. Nonetheless, searching for information to substitute the average DAD_{TRS} to study the correlation and to find origins of the correlations has been attempted. For example, in one research, the DAD_{PRC} distributions in the relatively stable productive reactant complexes (PRCs) in enzymes (narrowly distributed) and variants (more broadly distributed) were computed and used to substitute the DAD_{TRS} distributions to correlate with the corresponding ΔE_a's.[26] In others, secondary (2°) KIEs on the H/D position at or near the reaction centers have been used as a ruler for the crowdedness at the reaction centers or the tightness of the electronically associated TRS structures providing information for the relative density of of the DAD_{TRS} distributions.[34] Moreover, determination of the stable structures that mimic the PRCs of the enzymatic reactions have been used to provide information about the qualitative order of DAD_{TRS} magnitudes in wild-type enzymes and variants to correlate with the ΔE_a's.[32,45] We have also used similar methods to investigate such correlations for the hydride transfer reactions in solution.[39,40] While these have indirectly helped with understanding of the relationship between DAD_{TRS} and ΔE_a, a direct correlation between the two would be needed to effectively test the VA-AHT model or to help build future necessary models. To investigate the latter correlation, TRS structures for H-transfer reactions need to be obtained. That has, however, been difficult, due to the position uncertainty of the transferring H in the TRS structures.

In this paper, we developed a method to compute the TRS structures for H-transfer reactions defined in the VA-AHT model and attempted to directly correlate DAD_{TRS} with the observed temperature dependence of 1° KIEs (ΔE_a). The systems chosen to develop and test the method are the hydride transfer reactions from 1,3-dimethyl-2-phenylbenzimidazoline (DMPBIH) to 9-(para-substituted(*G*) phenyl)xanthylium ion (*G*PhXn$^+$) (eqn. 1). We have determined the ΔE_a's for these reactions in acetonitrile and found that an electron-withdrawing group (EWG) on *G*PhXn$^+$, as compared to an electron-donating group (EDG), gives rise to a smaller ΔE_a value.[40] For example, the ΔE_a's for the reactions of *G*PhXn$^+$ with G = CF_3, H, $N(CH_3)_2$ are 0.03, 0.27, and 0.50 kcal/mol, respectively. Together with the Υ-$2CH_3/2CD_3$ 2° KIEs on DMPBIH determined, we concluded that an EWG makes a tighter charge-transfer (CT) complex in the TRS leading to a smaller ΔE_a value, in agreement with the predictions from the VA-AHT model. Herein, we computed TRS structures for the reactions with three *G*PhXn$^+$ and calculated the Υ-2° KIEs for the corresponding TRS's of different DAD_{TRS}'s. These 2° KIEs were fitted to the observed ones to find the optimal TRS structures and DAD_{TRS}'s that the reactions would use. We found that the TRS with the CF_3 group has the shortest DAD_{TRS} and the one with $N(CH_3)_2$ has the longest DAD_{TRS}, directly confirming that a system with higher rigidity gives rise to a smaller ΔE_a. The hybridizations of the donor and acceptor carbons at the TRS's have been calculated to demonstrate the relationship between the position of TRS on the reaction coordinate and the exothermicity of the reactions. Our method can be used to calculate the TRS structures for similar H-transfer reactions and will provide a possibility to study the structure-reactivity relationship for nonclassical H-tunneling reactions and the nature of the TRS structures.

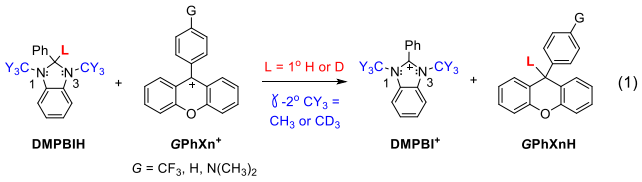

(1)

Computational Method Establishment

The VA-AHT model has been described in many publications including ours.[17,35,37,38,46] It involves two activation processes. In the first activation process, heavy atom motions bring the reactants (D-H and A) (again, D = Donor, A = Acceptor) to an activated transition state ([D-H---H-A]$^{\neq}$) in which the H wavefunctions from the potential wells of degenerate reactant [D-H]$^{\neq}$ and product [H-A]$^{\neq}$ are allowed to effectively overlap, *i.e.*, tunneling. This activated transition state is the TRS. The activation process involves motions of all atoms (from reactants as well as environment) except the transferring H. It accompanies orbital rehybridization and charge redistribution at the donor and acceptor, so it determines 2° KIEs. In the second activation process, the appropriately short DAD_{TRS}'s are sampled by heavy atom motions for H-tunneling to take place efficiently. The tunneling process is 1° H isotope sensitive and thus determines 1° KIEs.

To calculate 2° KIEs, the heavy atom framework structure of a TRS is needed. In literature, it has been approximately treated as the quantum superposition of activated degenerate classical reactant ([D-H A]$^{\neq}$) and product ([D H-A]$^{\neq}$) states that have the same heavy atom frame structures but different position of the transferring H.[14,38] Herein, we use the two computable structures for the purpose. Similar ways to calculate 2° KIEs have been used in literature including ours.[37,38,46] To compute such structures, we use classical TS structures as initial guesses to start. (In classical TS, H is partially bonded to both donor and acceptor, but in [D-H A]$^{\neq}$ and [D H-A]$^{\neq}$, H is fully bonded to either one.) Like a classical H-transfer reaction that can have multiple transition states (TS's), in principle, a H-tunneling reaction could have multiple TRS structures as well. For each TS structure, we pull the donor carbon and acceptor carbon apart to an assumed DAD, allowing the transferring H to stay with the donor carbon to generate the initial [D-H A]$^{\neq}$ geometry after relaxation, and allowing it to stay with the acceptor carbon to generate the initial [D H-A]$^{\neq}$ geometry after relaxation. We then construct the electronic potential energy surfaces (PES's) for the respective structures at the particular DAD by scanning dihedrals of the donor and acceptor carbons as two independent variables. The lowest intersection point of the two PES's is located and taken as the TRS of this DAD. Searching for TRS structures starting from other TS geometries and with other DAD's follow the same procedure.

Figure 1 delineates two PES's of [D-H A]$^{\neq}$ (in cyan color) and [D H-A]$^{\neq}$ (in pink color) for the hydride transfer reaction from DMPBIH to PhXn$^+$ at DAD_{TRS} = 3.2 Å (starting from the lowest energy classical TS geometry). The dihedrals ϕ and θ are with respect to the donor and acceptor carbons in both structures, respectively (see Figure 1 caption for detailed definitions). The

lowest energy intersection point of the two PES's is circled. That is the lowest energy TRS among the three found with DAD_{TRS} = 3.2 Å The corresponding [D-H A]$^{\neq}$ and [D H-A]$^{\neq}$ structures are given as structures **A** and **B** in Figure 1, respectively. Since searching for the intersection point focuses on finding the same dihedrals in the two structures (starting from the same classical TS geometry though) little difference in them would be expected. For one example, the relative positions of the two Ph groups at C-2 of DMPBIH and C-9 of $PhXn^+$ in structures **A** and **B** are slightly different.

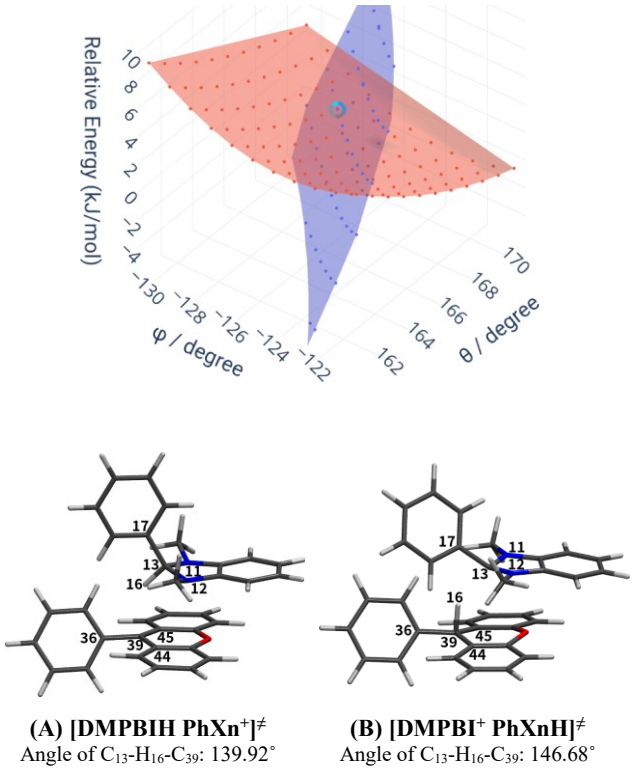

(A) [DMPBIH PhXn$^+$]$^{\neq}$
Angle of C_{13}-H_{16}-C_{39}: 139.92˚

(B) [DMPBI$^+$ PhXnH]$^{\neq}$
Angle of C_{13}-H_{16}-C_{39}: 146.68˚

Figure 1. The electronic PES scans as a function of dihedrals φ and θ for the activated complexes of reactants ([D-H A]$^{\neq}$,in cyan color) and products ([D H-A]$^{\neq}$,in pink color) (DAD_{TRS} = 3.2 Å) of the hydride-transfer reaction from DMPBIH to $PhXn^+$ (D-donor, A-acceptor). The lowest energy intersection point between the two PES's is taken as the TRS structure of this DAD (circled in the 3D figure), being a nonclassical hybrid structure of reactant state (**A**) and product state (**B**) (top: DMPBIH, bottom: $PhXn^+$) that are supposed to have the same heavy atom framework structure (see texts). The dihedral φ is defined by N11-N12-C13-C17 in DMPBIH, and the dihedral θ is defined by C44-C45-C39-C36 in $PhXn^+$. This is one of the three TRS's found with DAD_{TRS} = 3.2 Å (see Supporting Information for the atom coordinates of reactant and product structures of the TRS's), and is the most populated (lowest electronic energy) structure. In **A**, the transferring H-16 is at the donor C-13. In **B**, the transferring H-16 is at the acceptor C-39.

The TRS structures are used to calculate 2° KIEs. General procedures are as follows. (i) Calculate free energies ($G°$ = $G°_{electronic}$ + $G°_{vibrational}$) of the ground state (GS) reactants D-H, A^+, and two degenerate states of a TRS ([D-H A]$^{\neq}$ and [D H-A]$^{\neq}$); (ii) calculate two rate constants (k[TRS]'s) for system to reach the two TRS states (k[D-H A]$^{\neq}$ and k[D H-A]$^{\neq}$), respectively, using the Eyring equation (free energy of activation $\Delta G^{\neq} = G°_{TRS} - G°_{GS}$(D-H) - $G°_{GS}(A^+)$); (iii) take composite rate constant (k[TRS]) as the geometric mean of k[D-H A]$^{\neq}$ and k[D H-A]$^{\neq}$; (iv) calculate k[TRS] for reaction involving isotopes, here the 1,3-$2CD_3$ substitution in DMPBIH; and (v) calculate 2° KIE = k[TRS($2CH_3$)]/k[TRS ($2CD_3$)] on DMPBIH. Since each reaction has more than one TRS leading to more than one k[TRS] value (k[TRS]$_i$, i represents different TRS's), the overall KIE is calculated using eqn. 2 where n is the total number of TRS's at a certain DAD_{TRS}.

$$2° \text{ KIE} = \sum_n k[\text{TRS}(2\text{CH}_3)]_i / \sum_n k[\text{TRS}(2\text{CD}_3)]_i \quad (2)$$

For comparison, classical 2° KIEs were also calculated using eqn. 2. There, the optimized classical TS geometries were used.

The hybridization states (sp^H) of the donor and acceptor carbons in the TRS structure were calculated using eqn. 3.[37,38,46]

$$H = 2 + (180 - \theta)/(180 - \theta_0) \quad (3)$$

In this equation, θ is the out-of-plane bending angle at the TRS, θ_0 is the angle of the reduced form of each reactant.

Weight averaged hybridizations ($H(W)$'s) are calculated using eqn. 4.

$$H(W) = \sum_n p_i H_i \quad (4)$$

In this equation, p_i is the percentage of the individual TRS calculated using Boltzmann distribution of the average free energies (ε_i's) of the reactant- and product-state of the TRS (eqn. 5, $\varepsilon_i = (G°([\text{D-H A}]^{\neq}) + G°([\text{D H-A}]^{\neq})/2$, $k(B)$ is the Boltzmann constant), and H_i is the hybridization state of the donor or acceptor carbon of the corresponding TRS.

$$p_i = \frac{e^{-\varepsilon_i/k(B)T}}{\sum_n e^{-\varepsilon_i/k(B)T}} \quad (5)$$

We also calculated the weight averaged hybridizations for the classical TS's of the three reactions for comparison with those from the TRS's. Same procedures were followed and eqns. 3 – 5 were used.

Results and Discussion

Formation of the CT complexes between NADH/NAD^+ analogues have been well known.[40,47,48] In order to demonstrate the formation of the CT complexation in our systems, we also determined the ground state CT absorption band for the reaction of DMPBIH with a substituted GPhXn$^+$ as well as the disappearance of the CT band with time during the reaction. This information can be found in Supporting Information (Figure S1).

The ϒ-2° $2CH_3/2CD_3$ KIE on DMPBIH originates from the decrease in negative hyperconjugation between the lone-pair electrons on N and σ* orbital of the attached C-H/D bond, due to the loss of electron density on N during the reaction.[39,40,49,50] This decrease in negative hyperconjugation tightens the C-H/D bonds, leading to an inverse 2° KIE. Therefore, the 2° KIE reflects the change in charge density on DMPBIH during activation and thus could be used to suggest the tightness of the CT complexation. It is expected that an EWG on GPhXn$^+$ would make a tighter CT complex so that the DMPBIH moiety at TRS ends up with more electron density loss producing a more inverse 2° KIE. This is consistent with our observations. For example, the 2° KIEs for G = CF_3, H and $N(CH_3)_2$ are 0.89, 0.91 and 0.94, respectively.[40] These 2° KIEs are listed in Table 1 for a direct comparison with the calculated ones.

The calculated ϒ-2° $2CH_3/2CD_3$ KIEs following the VA-AHT model with TRS's of different DAD_{TRS}'s are listed in Table 1. The 2° KIEs calculated following the classical hydride transfer

mechanisms are also listed in the same table for comparison. We also located the corresponding productive reactive complexes (PRC's) by calculating the intrinsic reaction coordinates from the corresponding classical TS's.[39] The range of DAD_{PRC}'s for each of the reactions are 3.36 – 3.47 Å (for CF_3 substitution), 3.35 – 3.45 Å (H), and 3.33 – 3.49 Å ($N(CH_3)_2$). By examining the DAD_{PRC} ranges, it appears reasonable to assume that the activated TRS's would have a DAD_{TRS} no longer than 3.3 – 3.4 Å. All of the 2° KIEs calculated are inverse, which are consistent with the observations. The shortest DAD_{TRS} calculated for was 2.8 Å. That is because the much smaller 2° KIEs expected for the further shorter DAD_{TRS}'s (by inference from the trend of their change with DAD_{TRS} in Table 1) would not only deviate too much from the observed values but also very close to the corresponding 2° equilibrium isotope effect (EIE = 0.814[50]) for DMPBIH to be fully converted to its $DMPBI^+$ product. While the former is not hard to understand, the latter implicates that the DMPBI moiety at the TRS would carry a charge closer to +1. That would be less likely for a very exothermic process during which the transferring H would still be largely attached to the DMPBI structure at the early TRS according to Hammond's postulate. This would be especially true for the reaction of the CF_3 substitution. Therefore, we infer that the TRS's of the reactions in study would have DAD_{TRS}'s not significantly below the range from 2.8 to 3.4 Å. It should be noted that H-tunneling taking place at within this range of DAD_{TRS}'s has been reported in enzymes and solution.[37,38,46,51,52]

Table 1. Comparison of observed versus computed Υ-$2CH_3/2CD_3$ 2° KIEs on DMPBIH for its hydride transfer reactions with substituted *G*$PhXn^+$

	Obsd 2° KIE's[obs a]	Classical 2° KIEs[calcd]	Nonclassical 2° KIEs[calcd]			
G			at DAD_{TRS}			
			2.8 Å	3.0 Å	3.2 Å	3.4 Å
CF_3	0.89 (0.01)	0.870	0.829	0.859	0.872	0.890
H	0.91 (0.01)	0.877	0.836	0.864	0.892	0.915
$N(CH_3)_2$	0.94 (0.02)	0.859	0.840	0.880	0.898	0.887

[a] from ref [40], numbers in parentheses are standard deviations.

Substituent and DAD_{TRS} dependences of the computed Υ-2° KIE's on DMPBIH

From the reactions of *G*$PhXn^+$ with substituents CF_3 to H to $N(CH_3)_2$, the observed Υ-2° $2CH_3/2CD_3$ KIE on DMPBIH becomes less and less inverse, but the calculated 2° KIEs following the classical mechanism not only do not match with them in magnitudes but also show a slight opposite trend with the $N(CH_3)_2$ substitution giving the most inverse 2° KIE (Table 1). While the observed ΔE_a's of ~ 0 to 0.50 kcal/mol for the three reactions have already indicated that the hydride transfers take place by tunneling effect,[40] the differences further support the idea that these hydride transfer processes do not use the classical mechanism. Therefore, the substituent dependence of Υ-2° KIEs computed following the classical mechanism will not be discussed in this paper.

The 2° KIEs computed from the nonclassical TRS's following the VA-AHT model in Table 1 do show that they become less and less inverse from *G* = CF_3 to H to $N(CH_3)_2$ substitutions on *G*$PhXn^+$. This implicates that an EWG would make the DMPBIH moiety to have higher positive charge density developed at its TRS. While it is generally thought, according to Hammond's Postulate, that an EWG substitution would give rise to an earlier C-H cleavage activated complex on the reaction coordinate (more exergonic!) so that the corresponding reaction would accompany development of a lower density of positive charge on DMPBIH and thus result in a less inverse 2° KIE, the opposite order of the three 2° KIE values can only indicate that the charge redistribution during the reaction is largely resulted from CT complexation between the donor and acceptor. Therefore, an EWG makes a tighter CT complex resulting in more loss of electron density from DMPBIH producing a more inverse 2° KIE. The effect of the CT complex tightness on 2° KIEs can further be demonstrated by the findings that the computed 2° KIE values decrease, *i.e.*, become more inverse, as DAD_{TRS} decreases for all of the three reactions (Table 1). All together, the computed trends of 2° KIEs are consistent with our expectations that an EWG would make a tighter CT complex and thus a shorter DAD_{TRS}.[40] It should be noted that the increasing trend of 2° KIE values with increasing DAD_{TRS} for the reaction with $(CH_3)_2N$ substitution reaches its maximum at DAD_{TRS} = 3.2 Å, then becomes smaller at 3.4 Å. This suggests that the maximum DAD_{TRS} for the reaction of $(CH_3)_2NPhXn^+$ would be shorter than 3.4 Å.

Fit of the computed to observed 2° KIEs to find the DAD_{TRS}'s

The calculated 2° KIEs following the VA-AHT mechanisms are more inverse than the observed ones (Table 1). This could be resulted from experimental errors as well as approximations in our model/method and ways to locate the degenerate reactant and product structures. For the latter, errors could be from the slight difference of the two structures that we found and the step size of PES scans over the two dihedrals that we used to locate them (we used as small step size as possible.). Note that KIEs calculated with both the gas-phase and full enzyme conditions, using other tunneling models and other computation methods, were sometimes also found underestimated than the experimental ones for the hydride transfer reactions in dihydrofolate dehydrogenases from different sources.[53,54] Therefore, assigning a specific DAD_{TRS} to each system by directly matching the calculated with observed 2° KIEs appears not possible. However, a comparison of the observed 2° KIEs of the three reactions with those calculated as a function of both substituent and DAD_{TRS} could possibly differentiate the DAD_{TRS}'s that the reactions use. At first, the extent of increase in calculated 2° KIEs from *G* = CF_3 to H to $N(CH_3)_2$ in *G*$PhXn^+$ at *each* DAD_{TRS} is much smaller than that in the observed 2° KIEs (0.89, 0.91 and 0.94, respectively). This reasons that the three systems do not likely use the same DAD_{TRS}. While the change in calculated 2° KIEs with DAD_{TRS}'s could be much larger depending upon the ranges of DAD_{TRS}'s selected, a comparison of experiments with computations strongly suggest that DAD_{TRS}'s that the reactions use increase for the reactions of *G*$PhXn^+$ from G = CF_3 to H to $N(CH_3)_2$. By carefully comparing the observed 2° KIEs with the magnitudes of the calculated 2° KIEs as well as the substituent and DAD_{TRS} dependencies of the calculated 2° KIEs for three reactions, we find that TRS's with DAD_{TRS}'s within ~2.8 - 3.0 Å for G = CF_3, 3.0 – 3.2 Å for H, and around 3.2 Å for $N(CH_3)_2$, would better fit to the observations. For example, the 2° KIEs calculated for three TRS's in this work are 0.83 (for CF_3 at 2.8 Å), 0.86 (H at 3.0 Å), and 0.90 ($N(CH_3)_2$ at 3.2 Å), being closer to the observed KIE trends. While the 2° KIE differences of about 0.05 between calculations and experiments appear large, a closer fit to the calculations may be found when calculations are further done with more DAD_{TRS}'s of smaller increments. For example, we also calculated the 2° KIE for the reaction with $N(CH_3)_2$ substitution at DAD_{TRS} of 3.3 Å and found it to be 0.904 (not included in Table 1, but can be seen in the subsequent Figure 3 and Table 2), closer to the experimental value as compared to 0.898 at DAD_{TRS} = 3.2 Å. Nevertheless, matching of the trend of 2° KIEs in three reactions between calculations and experiments reveals that reaction with an EWG gives a shorter DAD_{TRS} than that with an EDG.

The results are consistent with our expectation that the average DAD_{TRS}'s are in order of reactions with CF_3 < H < $N(CH_3)_2$ substitutions.[40] In the CT complexes between donors and acceptors,

it is expected that a shorter DAD_{TRS} reflects stronger CT complexation and thus stronger donor-acceptor attracting vibrations to sample narrower DAD_{TRS} distributions.[34] A comparison of the DAD_{TRS} order with the observed corresponding ΔE_a's supports the prediction from the VA-AHT model, *i.e.*, a smaller DAD_{TRS} and narrower distribution of DAD_{TRS}'s gives rise to a weaker temperature dependence of 1° KIEs.

Bent TRS geometries and rehybridization processes

The reactant state ($[D\text{-}H\ A]^{\neq}$) and product state ($[D\ A\text{-}H]^{\neq}$) structures of the most stable TRS's for the reactions of CF_3PhXn^+ (DAD_{TRS} = 3.0 Å) and $(CH_3)_2NPhXn^+$ (3.3 Å) are included in Figures 2 and 3. Together with such a TRS structure for the reaction of $PhXn^+$ shown in Figure 1, it can be seen that all of the TRS structures have bent geometries (with nonlinear C_D-H-C_A angles). We have attempted to compute the TRS structures by imposing a linear C_D-H-C_A restriction but found the "linear" structures are not realistic, with free energies being much higher than that of the corresponding bent TRS (for one example, about 4.8 kcal/mol higher in electronic energy, see Supplemental Information Figure S3 and energy comparison in Table S2). The weight averaged hybridizations at the donor and acceptor carbons computed from classical TS's and optimal-fit TRS's for CF_3 and $(CH_3)_2N$ substitutions are listed in Table 2 in order to discuss about the relative positions of TRS's in the reaction coordinate as well as orbital requirements for H-tunneling to take place. Since these reactions are very exergonic (for example, the $\Delta G°$ for the reaction with $PhXn^+$ in acetonitrile is – 42.4 kcal/mol[55]), according to Hammond's Postulate, the TS's/TRS's would be very reactant-like. That is, the donor and acceptor carbon hybridizations at TRS's would be closer to sp^3 and sp^2, respectively. The hybridization results in Table 2 show that the hybridizations of the donor carbon for the reactions of CF_3 and $N(CH_3)_2$ substitutions ($sp^{>2.90}$) are indeed closer to sp^3 but those of the acceptor carbon for the reactions of CF_3 and $N(CH_3)_2$ ($sp^{>2.67}$) substitutions are very far away from sp^2. The nonsynchronous rehybridizations at donor and acceptor have been found in many H-tunneling reactions in both solution and enzymes.[37,38,46,56] The sum of the two hybridizations often being larger than 5 ($sp^{>5}$) suggests a requirement of extra orbital preparations at the donor/acceptor for H-tunneling to take place. Here in our case, the extra orbital preparation mainly happens at the acceptor C. This is consistent with the findings in the hydride transfer reaction of NAD(P)H catalyzed by a dihydrofolate reductase – the hybridization of the acceptor at the tunneling TS resembles the product.[56] On the other hand, it is interesting to find that rehybridizations at donor and acceptor carbons are also nonsynchronous for the classical process (see Table 2). We regard that the nonsynchronous rehybridization in the latter classical mechanism is resulted from the CT complexation requirement in addition to the classical C-H cleavage process. Nevertheless, the extra orbital adjustment requirement for the classical transfer is

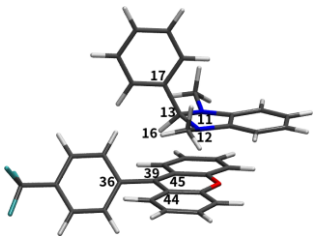

Angle of C_{13}-H_{16}-C_{39}: 144.96°

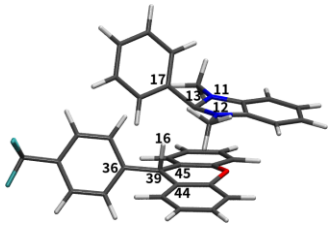

Angle of C_{13}-H_{16}-C_{39}: 156.32°

Figure 2. The reactant state $[D\text{-}H\ A]^{\neq}$ (left) and product state $[D\ H\text{-}A]^{\neq}$ (right) of the most stable TRS with DAD = 3.0 Å for the reaction of CF_3PhXn^+ with DMPBIH. The CF_3PhXn moiety is at the bottom and the DMPBI moiety is on the top. The donor carbon, transferring H and acceptor carbon were numbered as C13, H16 and C39, respectively.

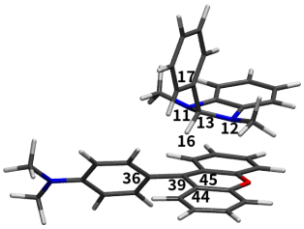

Angle of C_{13}-H_{16}-C_{39}: 139.92°

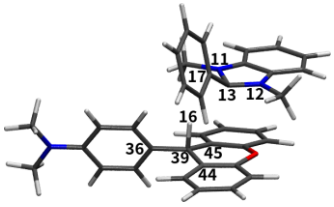

Angle of C_{13}-H_{16}-C_{39}: 104.32°

Figure 3. The reactant state $[D\text{-}H\ A]^{\neq}$ (left) and product state $[D\ H\text{-}A]^{\neq}$ (right) of the most stable TRS with DAD = 3.3 Å for the reaction of $(CH_3)_2NPhXn^+$ with DMPBIH. The $(CH_3)_2NPhXn$ moiety is at the bottom and the DMPBI moiety is on the top. The donor carbon, transferring H and acceptor carbon were numbered as C13, H16 and C39, respectively.

much less than that for the tunneling process. Furthermore, it appears that slightly more rehybridization at the donor and slightly less rehybridization at the acceptor are needed for the tunneling reaction of $N(CH_3)_2$ substitution than CF_3 substitution (Table 2). According to Hammond's Postulate, however, the rehybridization on both donor and acceptor would be more in the former reaction than in the latter. While this seems the case for the classical activation processes (Table 2, although not significant), the position of the H-tunneling TRS in the reaction coordinate in terms of rehybridizations would not be able to be predicted by Hammond's Postulate.[56]

Table 2. The weight averaged hybridizations ($sp^{H(W)}$) of the donor and acceptor carbons at the classical TS's and optimal-fit TRS's of the reactions of DMPBIH with CF_3PhXn^+ and $(CH_3)_2NPhXn^+$

		CF_3PhXn^+		$(CH_3)_2NPhXn^+$	
TS's	Donor C	$sp^{2.88}$		$sp^{2.86}$	
	Acceptor C	$sp^{2.46}$		$sp^{2.48}$	
TRS's		DAD_{TRS} Range[a]		DAD_{TRS} Range[a]	
		2.8 Å	3.0 Å	3.2 Å	3.3 Å
	Donor C	$sp^{2.98}$	$sp^{2.94}$	$sp^{2.92}$	$sp^{2.90}$
	Acceptor C	$sp^{2.74}$	$sp^{2.77}$	$sp^{2.67}$	$sp^{2.70}$

[a] The average DAD_{TRS} is expected to be within this range, as discussed in the preceding section.

Conclusions

A method to compute TRS structures for H-tunneling reactions was established. The TRS was treated as a linear combination of the degenerate activated reactant and product vibrational states. It was applied to calculate the TRS structures with different DAD_{TRS}'s for hydride transfer reactions from DMPBIH to *G*$PhXn^+$. The Ƴ-$2CH_3/2CD_3$ 2° KIEs on DMPBIH were calculated and fitted to the observed 2° KIEs to give rise to the possible TRS structure and DAD_{TRS} that each reaction uses. All of the TRS's have bent geometries with orbital hybridization at the acceptor carbon far more advanced than predicted from a classical mechanism. The latter are also consistent with the literature findings, implicating that extra orbital adjustments are needed for a nonclassical H-tunneling to take place. The optimal-fit DAD_{TRS}'s for the reactions of CF_3, H, and $(CH_3)_2N$ substitutions are likely in the ranges of ~2.8 - 3.0 Å, 3.0 - 3.2 Å, and 3.2 – 3.3 Å, respectively.

Although an exact DAD_{TRS} for each reaction could not be given, results clearly show that the order of reaction center rigidity of the three reactions caused by the donor-acceptor CT attracting vibrations is $TRS(CF_3) > TRS(H) > TRS((CH_3)_2N)$. A correlation of the DAD_{TRS}'s with the observed temperature dependence of 1° KIEs (reflected by ΔE_a's) indicates that the more rigid reaction centers at the TRS give rise to a smaller ΔE_a. These are consistent with explanations for the recently frequently observed temperature independence of 1° KIEs in enzymes and temperature dependence of 1° KIEs in variants using the VA-AHT model. That is, enzymes have well organized reaction coordinate with constructive protein vibrations more likely making a TRS of rigid reaction centers, whereas in the variants protein packing effect is impaired, leading to alternate positions for the binding of substrate and enhanced DAD_{TRS} sampling at the TRS. Our results from solution reactions, together with those from enzymes, showcase a new structure - ΔE_a relationship. While this relationship is consistent with the VA-AHT model, we cannot exclude the possibility that our results could also be fitted to other contemporary H-transfer/tunneling models. Nonetheless, a *systematic* study of the structure - ΔE_a relationship will certainly add to the current debates on the appropriateness of models to describe H-transfer reactions in enzymes and solution as well as provide information to develop future necessary H-transfer models.[12-14,18,36,57,58]

Computational methods

All of the calculations were performed under the M06-2X[2]/Def2-SVP[3] level of theory with fine DFT integration grid in Gaussian 09 software. A frequency scaling factor of 0.9687 is used to minimize the overestimation error of the harmonic model.[39] The PES intersecting diagram is created by using Ploty Online Chart Studio [https://chart-studio.plotly.com].

ASSOCIATED CONTENT

Supporting Information

The ground state charge-transfer absorption and its changes with time for the reaction of DMPBIH with a $G\text{PhXn}^+$, the atom coordinates and the electronic and free energies of the classical TS's and nonclassical TRS's. This material is available free of charge via the Internet at http://pubs.acs.org.

AUTHOR INFORMATION

Corresponding Author

* yulu@siue.edu

Notes

The authors declare no competing financial interests.

ACKNOWLEDGMENT

Acknowledgment is made to the donors of the National Science Foundation (NSF# 1800194) for supporting of this research. HPC cluster support from computations from Southern Illinois University Edwardsville (SIUE) is also acknowledged. The cluster is related to the SIUE Campus Cluster Project funded by the National Science Foundation Campus Cyberinfrastructure Program (NSF# 2018551). This paper is also dedicated to the memory of Dr. James E. Eilers who sadly passed away on March 12, 2021. Dr. Eilers was a computational chemist from SIUE and was a co-principal investigator of the first NSF grant acknowledged above. Y.L. specially thanks Dr. Eilers' help for starting his computational project and lab at SIUE, co-advising his students, as well as providing insightful discussions in his computational research, which happened both in Dr. Eilers' tenure at SIUE and after his retirement.

REFERENCES

(1) Bell, R. P.: *The tunnel effect in chemistry*; Chapman & Hall: London & New York., 1980.

(2) Stojković, V.; Kohen, A.: Enzymatic H-transfer: Quantum tunneling and coupled motion from kinetic isotope effects. *Isr. J. Chem.* **2009**, *49*, 163-173.

(3) Kim, Y.; Kreevoy, M. M.: The experimental manifestations of corner-cutting tunneling. *J. Am. Chem. Soc.* **1992**, *114*, 7116-7123.

(4) Kreevoy, M. M.; Ostovic, D.; Truhlar, D. G.; Garrett, B. C.: Phenomenological manifestations of large-curvature tunneling in hydride-transfer reactions. *J. Phys. Chem.* **1986**, *90*, 3766-3774.

(5) Kwart, H.: Temperature dependence of primary kinetic isotope effect as a mechanistic criterion. *Acc. Chem. Res.* **1982**, *15*, 401-408.

(6) Powell, M. F.; Bruice, T. C.: Effect of isotope scrambling and tunneling on the kinetic and product isotope effects for reduced nicotinamide adenine dinucleotide model hydride transfer reactions. *J. Am. Chem. Soc.* **1983**, *105*, 7139–7149.

(7) Nesheim, J. C.; Lipscomb, J. D.: Large kinetic isotope effects in methane oxidation catalyzed by methane monooxygenase: Evidence for C-H bond cleavage in a reaction cycle intermediate. *Biochemistry* **1996**, *35*, 10240-10247.

(8) Rickert, K. W.; Klinman, J. P.: Nature of hydrogen transfer in soybean lipoxygenase 1: separation of primary and secondary isotope effects. *Biochemistry* **1999**, *38*, 12218-12228.

(9) Basran, J.; Sutcliffe, M. J.; Scrutton, N. S.: Enzymatic H-Transfer Requires Vibration-Driven Extreme Tunneling. *Biochemistry* **1999**, *38*, 3218-3222.

(10) Kohen, A.; Cannio, R.; Bartolucci, S.; Klinman, J. P.: Enzyme dynamics and hydrogen tunnelling in a thermophilic alcohol dehydrogenase. *Nature* **1999**, *399*, 496-499.

(11) Knapp, M. J.; Rickert, K.; Klinman, J. P.: Temperature-dependent isotope effects in soybean lipoxygenase-1: Correlating hydrogen tunneling with protein dynamics. *J. Am. Chem. Soc.* **2002**, *124*, 3865-3874.

(12) Nagel, Z. D.; Klinman, J. P.: Update 1 of: Tunneling and dynamics in enzymatic hydride transfer. *Chem. Rev.* **2010**, *110*, PR41–PR67.

(13) Truhlar, G. D.: Tunneling in enzymatic and nonenzymatic hydrogen transfer reactions. *J. Phy. Org. Chem.* **2010**, *23*, 660-676.

(14) Layfield, J. P.; Hammes-Schiffer, S.: Hydrogen Tunneling in Enzymes and Biomimetic Models. *Chem. Rev.* **2014**, *114*, 3466–3494.

(15) Bae, S. H.; Li, X.-X.; Seo, M. S.; Lee, Y.-M.; Fukuzumi, S.; Nam, W.: Tunneling Controls the Reaction Pathway in the Deformylation of Aldehydes by a Nonheme Iron(III)–Hydroperoxo Complex: Hydrogen Atom Abstraction versus Nucleophilic Addition. *J Am Chem Soc* **2019**, *141*, 7675–7679.

(16) Zhang, J.; Yang, J.-D.; Cheng, J.-P.: Diazaphosphinanes as hydride, hydrogen atom, proton or electron donors under transition-metal-free conditions: thermodynamics, kinetics, and synthetic applications. *Chem. Sci.* **2020**, *11*, 3672-3679.

(17) Roston, D.; Kohen, A.: A Critical Test of the "Tunneling and Coupled Motion" Concept in Enzymatic Alcohol Oxidation. *J. Am. Chem. Soc.* **2013**, *135*, 13624–13627.

(18) Klinman, J. P.; Offenbacher, A. R.: Understanding Biological Hydrogen Transfer Through the Lens of Temperature Dependent Kinetic Isotope Effects. *Acc. Chem. Res.* **2018**, *51*, 1966–1974.

(19) Sikorski, R. S.; Wang, L.; Markham, K. A.; Rajagopalan, P. T. R.; Benkovic, S. J.; Kohen, A.: Tunneling and coupled motion in the *E. coli* dihydrofolate reductase catalysis. *J. Am. Chem. Soc.* **2004**, *126*, 4778-4779.

(20) Schowen, R. L.: The strengths and weaknesses of model reactions for the assessment of tunneting in enzymatic reactions. In *Quantum tunnelling in enzyme catalyzed reactions*; Allemann, R., Scrutton, N., Eds.; Royal Society of Chemistry: London, UK, 2009; Vol. CH. 13; pp 292-313.

(21) Francisco, W. A.; Knapp, M. J.; Blackburn, N. J.; Klinman, J. P.: Hydrogen tunneling in peptidylglycine-hydroxylating monooxygenase. *J. Am. Chem. Soc.* **2002**, *124*, 8194-8195.

(22) Knapp, M. J.; Klinman, J. P.: Environmentally coupled hydrogen tunneling. Linking catalysis to dynamics. *Eur. J. Biochem.* **2002**, *269*, 3113–3121.

(23) Maglia, G.; Allemann, R. K.: Evidence for environmentally coupled hydrogen tunneling during dihydrofolate reductase catalysis. *J. Am. Chem. Soc.* **2003**, *125*, 13372-13373.

(24) Basran, J.; Sutcliffe, M. J.; Scrutton, N. S.: Deuterium Isotope Effects during Carbon–Hydrogen Bond Cleavage by Trimethylamine Dehydrogenase: Implications for mechanism and vibrationally assisted hydrogen tunneling in wild-type and mutant enzymes. *J. Biol. Chem.* **2001**, *276*, 24581-24587.

(25) Harris, R. J., Meskys, R., Sutcliffe, M. J., Scrutton, N. S.: Kinetic Studies of the Mechanism of Carbon−Hydrogen Bond Breakage by the Heterotetrameric Sarcosine Oxidase of Arthrobacter sp. 1-IN. *Biochemistry* **2000** *39*, 1189-1198.

(26) Stojkoviç, V., Perissinotti, L., Willmer, D., Benkovic, S., and Kohen, A.: Effects of the donor acceptor distance and dynamics on hydride tunneling in the dihydrofolate reductase catalyzed reaction. *J. Am. Chem. Soc.* **2012**, *134*, 1738-1745.

(27) Wang, L.; Goodey, N. m.; Benkovic, S. J.; Kohen, A.: Coordinated effects of distal mutations on environmentally coupled tunneling in dihydrofolate reductase. *Proc. Nat. Acad. Sci. USA* **2006**, *103*, 15753-15758.

(28) Wang, Z.; Kohen, A.: Thymidylate synthase catalyzed H-transfers: Two chapters in one tale. *J. Am. Chem. Soc.* **2010**, *132*, 9820–9825.

(29) Romero, E.; Ladani, S. T.; Hamelberg, D.; Gadda, G.: Solvent-Slaved Motions in the Hydride Tunneling Reaction Catalyzed by Human Glycolate Oxidase. *ACS Catal.* **2016**, *6*, 2113−2120.

(30) Hu, S.; Soudackov, A. V.; Hammes-Schiffer, S.; Klinman, J. P.: Enhanced Rigidification within a Double Mutant of Soybean Lipoxygenase Provides Experimental Support for Vibronically Nonadiabatic Proton-Coupled Electron Transfer Models. *ACS Catal.* **2017**, *7*, 3569−3574.

(31) Howe, G. W.; van der Donk, W. A.: Temperature-Independent Kinetic Isotope Effects as Evidence for a Marcus-like Model of Hydride Tunneling in Phosphite Dehydrogenase. *Biochemistry* **2019**, *58*, 4260-4268.

(32) Pagano, P.; Guo, Q.; Ranasinghe, C.; Schroeder, E.; Robben, K.; Häse, F.; Ye, H.; Wickersham, K.; Aspuru-Guzik, A.; Major, D. T.; Gakhar, L.; Kohen, A.; Cheatum, C. M.: Oscillatory Active-Site Motions Correlate with Kinetic Isotope Effects in Formate Dehydrogenase. *ACS Catal.* **2019**, *9*, 11199−11206.

(33) Kuznetsov, A. M.; Ulstrup, J.: Proton and hydrogen atom tunneling in hydrolytic and redox enzyme catalysis. *Can. J. Chem.* **1999**, *77*, 1085-1096.

(34) Pudney, C. R. J., L.; Sutcliffe, M. J.; Hay, S.; Scrutton N. S. : Direct Analysis of Donor-Acceptor Distance and Relationship to Isotope Effects and the Force Constant for Barrier Compression in Enzymatic H-Tunneling Reactions. *J. Am. Chem. Soc.* **2010**, *132*, 11329-11335.

(35) Liu, Q.; Zhao, Y.; Hammann, B.; Eilers, J.; Lu, Y.; Kohen, A.: A Model Reaction Assesses Contribution of H-Tunneling and Coupled Motions to Enzyme Catalysis. *J. Org. Chem.* **2012**, *77*, 6825–6833.

(36) Kohen, A.: Role of Dynamics in Enzyme Catalysis: Substantial vs. Semantic Controversies. *Acc. Chem. Res.* **2015**, *48*, 466-473.

(37) Derakhshani-Molayousefi, M.; Kashefolgheta, S.; Eilers, J. E.; Lu, Y.: Computational Replication of the Primary Isotope Dependence of Secondary Kinetic Isotope Effects in Solution Hydride-Transfer Reactions: Supporting the Isotopically Different Tunneling Ready State Conformations. *J. Phys. Chem. A* **2016**, *120*, 4277−4284.

(38) Roston, D.; Kohen, A.: Elusive transition state of alcohol dehydrogenase unveiled. *Proc. Nat. Acad. Sci. USA* **2010**, *107*, 9572-9577.

(39) Lu, Y.; Wilhelm, S.; Bai, M.; Maness, P.; Ma, L.: Replication of the Enzymatic Temperature Dependency of the Primary Hydride Kinetic Isotope Effects in Solution: Caused by the Protein Controlled Rigidity of the Donor-Acceptor Centers? *Biochemistry* **2019**, *58*, 4035–4046.

(40) Maness, P.; Koirala, S.; Adhikari, P.; Salimraftar, N.; Lu, Y.: Substituent Effects on Temperature Dependence of Kinetic Isotope Effects in Hydride-Transfer Reactions of NADH/NAD+ Analogues in Solution: Reaction Center Rigidity Is the Key. *Org. Lett.* **2020**, *22*, 5963–5967.

(41) Hatcher, E.; Soudackov, A. V.; Hammes-Schiffer, S.: Proton-coupled electron transfer in soybean lipoxygenase. *J. Am. Chem. Soc.* **2004**, *126*, 5763-5775.

(42) Hatcher, E.; Soudackov, A. V.; Hammes-Schiffer, A.: Proton-Coupled Electron Transfer in Soybean Lipoxygenase: Dynamical Behavior and Temperature Dependence of Kinetic Isotope Effects. *J. Am. Chem. Soc.* **2007**, *129*, 187–196.

(43) Kamerlin, S. C. L.; Warshel, A.: An analysis of all the relevant facts and arguments indicates that enzyme catalysis does not involve large contributions from nuclear tunneling. *J. Phy. Org. Chem.* **2010**, *23*, 677-684.

(44) Kanaan, N.; Ferrer, S.; Martí, S.; Garcia-Viloca, M.; Kohen, A.; Moliner, V.: Temperature Dependence of the Kinetic Isotope Effects in Thymidylate Synthase. A Theoretical Study. *J. Am. Chem. Soc.* **2011**, *133*, 6692–6702.

(45) Horitani, M.; Offenbacher, A. R.; Carr, C. A. M.; Yu, T.; Hoeke, V.; Cutsail, G. E.; Hammes-Schiffer, S.; Klinman, J. P.; Hoffman, B. M.: C-13 ENDOR Spectroscopy of Lipoxygenase-Substrate Complexes Reveals the Structural Basis for C-H Activation by Tunneling. *J. Am. Chem. Soc.* **2017**, *139*, 1984−1997.

(46) Kashefolgheta, S.; Razzaghi, M.; Hammann, B.; Eilers, J.; Roston, D.; Lu, Y.: Computational Replication of the Abnormal Secondary Kinetic Isotope Effects in a Hydride Transfer Reaction in Solution with a Motion Assisted H-Tunneling Model. *J. Org. Chem.* **2014**, *79*, 1989-1994.

(47) Lu, Y.; Zhao, Y.; Handoo, K. L.; Parker, V. D.: Hydride-exchange reactions between NADH and NAD+ model compounds under non-steady-state conditions. Apparent and Real kinetic isotope effects. *Org. Biomol. Chem.* **2003**, *1*, 173 - 181.

(48) Fukuzumi, S.; Ohkubo, K.; Tokuda, Y.; Suenobu, T.: Hydride Transfer from 9-Substituted 10-Methyl-9,10-dihydroacridines to Hydride Acceptors via Charge-Transfer Complexes and Sequential Electron-Proton-Electron Transfer. A Negative Temperature Dependence of the Rates. *J. Am. Chem. Soc.* **2000**, *122*, 4286-4294.

(49) Perrin, C. L.; Ohta, B. K.; Kuperman, J.; Liberman, J.; Erdelyi, M.: Stereochemistry of Beta-Deuterium Isotope Effects on Amine Basicity. *J. Am. Chem. Soc.* **2005**, *127*, 9641-9647.

(50) Ma, L.; Sakhaee, N.; Jafari, S.; Wilhelm, S.; Rahmani, P.; Lu, Y.: Imbalanced Transition States from α-H/D and Remote β-Type N-CH/D Secondary Kinetic Isotope Effects on the NADH/NAD+ Analogues in Their Hydride Tunneling Reactions in Solution. *J. Org. Chem.* **2019**, *84*, 5431–5439.

(51) Webb, S. P.; Agarwal , P. K.; Hammes-Schiffer, S.: Combining Electronic Structure Methods with the Calculation of Hydrogen Vibrational Wavefunctions: Application to Hydride Transfer in Liver Alcohol Dehydrogenase. *J. Phys. Chem. B* **2000**, *104*, 8884–8894.

(52) Meyer, M. P.; Klinman, J. P.: Modeling temperature dependent kinetic isotope effects for hydrogen transfer in a series of soybean lipoxygenase mutants: The effect of anharmonicity upon transfer distance. *Chem Phys* **2005**, *319*, 283–296.

(53) R., M. A.; Major, D. T.: Temperature-Dependent Kinetic Isotope Effects in R67 Dihydrofolate Reductase from Path-Integral Simulations. *J. Phys. Chem. B* **2021**, *125*, 1369–1377.

(54) Pu, J.; Ma, S.; Gao, J.; Truhlar, D. G.: Small temperature dependence of the kinetic isotope effect for the hydride transfer reaction catalyzed by Escherichia coli dihydrofolate reductase. *J. Phys. Chem. B* **2005**, *109*, 8551−8556.

(55) Zhu, X. Q.; Deng, F. H.; Yang, J. D.; Li, X. T.; Chen, Q.; Lei, N. P.; Meng, F. K.; Zhao, X. P.; Han, S. H.; Hao, E. J.; Mu, Y. Y.: A classical but new kinetic equation for hydride transfer reactions. *Org. Biomol. Chem.* **2013**, *11*, 6071-6089.

(56) Pu, J.; Ma, S.; Garcia-Viloca, M.; Gao, J.; Truhlar, D. J.; Kohen, A.: Nonperfect Synchronization of Reaction Center Rehybridization in the Transition State of the Hydride Transfer Catalyzed by Dihydrofolate Reductase. *J. Am. Chem. Soc.* **2005**, *127*, 14879-14886.

(57) Masgrau, L.; Truhlar, D. G.: The Importance of Ensemble Averaging in Enzyme Kinetics. *Acc. Chem. Res.* **2015**, *48*, 431-438.

(58) Fan, Y.; Cembran, A.; Ma, S.; Gao, J.: Connecting Protein Conformational Dynamics with Catalytic Function As Illustrated in Dihydrofolate Reductase. *Biochemistry* **2013**, *52*, 2036-2049.

Graphical Table of Contents

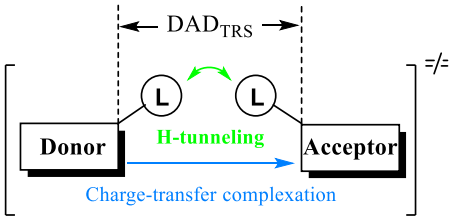

(L = H or D)

The longer the DAD$_{TRS}$

The larger the (E_{aD} - E_{aH})